Supporting information

Structural Analysis of Potassium Borate Solutions

Fayan Zhu[1,2], Daniel Bowron[2], Sabrina Gaertner[2,a], Chunhui Fang[1], Yongquan Zhou[1], Hongyan Liu[1], Alex C. Hannon[2*]

[1] Qinghai Institute of Salt Lakes, Chinese Academy of Sciences, Xining 81008

[2] ISIS Facility, STFC, Rutherford Appleton Laboratory, Chilton, Didcot, Oxon OX11 0QX, UK

[a]Current address: Miltenyi Biotec B.V. & Co. KG, (R&D Engineering, Biophysics), Friedrich-Ebert-Straße 68, 51429 Bergisch Gladbach, Germany

*Correspondence e-mail: alex.hannon@stfc.ac.uk

1 Sample Preparation

1.1 Reagents

$H_3{}^{11}BO_3$ was purchased from Sigma-Aldrich, and KOH was purchased from Fisher Scientific.

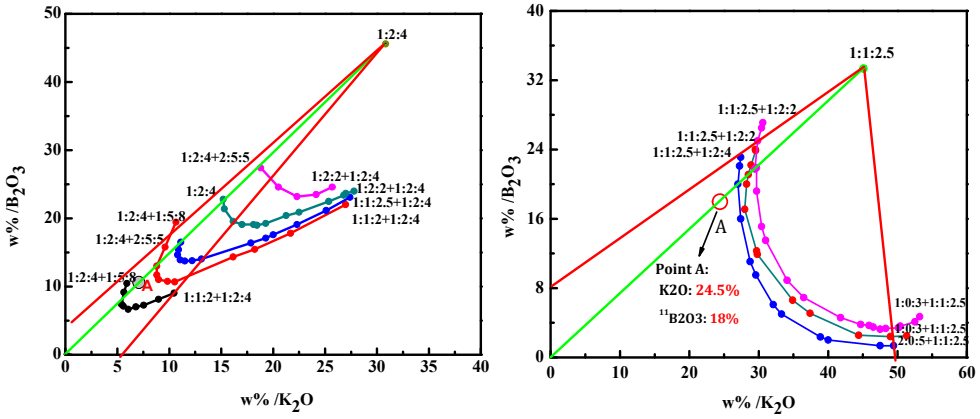

Figure S1 Ternary phase diagram of K_2O-B_2O_3-H_2O.

Left, potassium tetraborate phase; right, potassium metaborate phase

1.2 Preparation of Hydrous $K_2{}^{11}B_4O_7{\cdot}4H_2O$ and $K^{11}BO_2{\cdot}1.33H_2O$ Crystals

According to the phase diagram[S1] (Figure S1, left), the composition of point A is 7.1% K_2O, 10.5% B_2O_3. If we prepare 200g of $K_2[B_4O_5(OH)_4]$ solution, the mass of KOH and $H_3{}^{11}BO_3$ are as follows:

K_2O	~	2KOH	$^{11}B_2O_3$	~	$2H_3{}^{11}BO_3$
94.2		2×56.1	70		2×62
14.2		x=16.9 (g)	10.5×2		y=37.2 (g)

So we need 16.9 (g) KOH, 37.2 (g) $H_3{}^{11}BO_3$ to prepare $K_2{}^{11}B_4O_7 \cdot (4H_2O)$ crystal.

As shown in Figure S1 (right), the composition of point A is 24.5% K_2O, 18% $^{11}B_2O_3$. If we prepare 100g of KBO_2 solution, the required masses of KOH and H_3BO_3 are as follows:

K_2O	~	2KOH	$^{11}B_2O_3$	~	$2H_3{}^{11}BO_3$
94.2		2×56.1	70		2×62
24.5		x=29.2 (g)	18		y=32 (g)

So we need 29.2 (g) KOH, 32 (g) $H_3{}^{11}BO_3$ to prepare $K^{11}BO_2(\cdot 1.33H_2O)$ crystal.

The actual weight of KOH and $H_3{}^{11}BO_3$ are shown in Table S1.

Table S1 Weight (grams) of KOH, $H_3{}^{11}BO_3$ and H_2O for preparing borate crystals

	m_{KOH} (g)	$m_{H3^{11}BO3}$ (g)	m_{H2O} (g)
$K_2{}^{11}B_4O_7$ solution	21.3*	37.4**	240
$K^{11}BO_2$ solution	34.5*	32.0	99

*: the percentage composition of KOH ≥85%, so the actual mass of KOH was calculated by dividing by 0.85.

**: the theoretical value is 37.2 (g), but 37.4 (g) $H_3{}^{11}BO_3$ was actually weighted.

The solutions were prepared in a glass beaker, and then gently heated for several minutes to allow the hydrous $K_2{}^{11}B_4O_7{\cdot}4H_2O$ and $K^{11}BO_2{\cdot}1.33H_2O$ crystals to precipitate out. After this, the precipitated crystals were allowed to dry in air for two to three hours, and then they were ground to powder using a mortar and pestle.

1.3 Preparation of Anhydrous $K_2{}^{11}B_4O_7$ and $K^{11}BO_2$ crystals

Figure S2 shows TGA and DSC measurements made on non-isotopic samples of the hydrous crystals $K_2B_4O_7{\cdot}4H_2O$ and $KBO_2{\cdot}1.33H_2O$, using a Netzsch STA 449 F3 synchronous thermal analyzer. We assumed that the thermal behaviour of samples made with ^{11}B does not differ significantly, and the procedures used to dehydrate the hydrous crystals $K_2{}^{11}B_4O_7{\cdot}4H_2O$ and $K^{11}BO_2{\cdot}1.33H_2O$ are based on these TGA and DSC measurements. The TGA trace for $KBO_2.1.33H_2O$ shows evidence of rapid partial dehydration (maybe $KBO_2.1.33H_2O$ → $KBO_2.0.33H_2O$) occurring at 160 °C, followed by complete dehydration at ~206 °C. The behaviour of $K_2B_4O_7{\cdot}4H_2O$ is very different; dehydration begins at a temperature close to 100 °C, but proceeds very slowly and is not complete until a temperature ~400 °C. The DSC trace shows evidence of an exothermic event at ~550 °C, and so this temperature was used to ensure that this sample was dried thoroughly.

Firstly, the solutions were put into a furnace at 170 °C for 2 hours to remove most of the water of crystallisation, and then the temperature was increased (to 208 °C for $K^{11}BO_2{\cdot}1.33H_2O$, and to 550 °C for $K_2{}^{11}B_4O_7{\cdot}4H_2O$) to complete the dehydration process. The samples were removed from the furnace every two hours to check the weight loss. The details are shown in Table S2. The penultimate column of Table S2 shows the mass loss as a fraction of the initial sample mass, whilst the final column shows the theoretical fraction of the mass of each hydrous crystal that is H_2O. The values in these columns are evidence that

the crystals were thoroughly dehydrated. The fractional mass loss is not expected to be exactly the same as the theoretical value, firstly due to the possible presence of residual liquid water. Furthermore, for $K_2{}^{11}B_4O_7{\cdot}4H_2O$ there was a serious agglomeration at 170 ℃, producing a bubble in the crucible, and hence the crucible was removed from the furnace and the agglomeration was ground to a powder; there was the possibility of mass loss during this process.

Table S2 The mass of porcelain crucibles (cru.) and samples (samp.) during the dehydration process

Cru. number	Empty cru. (g)	Cru. + samp. (g)	Cru. + samp. during dehydration process (g)				*	**
			170 ℃	550℃	550℃	550℃		
			$K_2{}^{11}B_4O_7{\cdot}4H_2O$					
1	28.6213	31.0766	30.4944	30.5061	30.4937	30.4922	0.2076	0.2349
2	29.4853	32.1485	31.5150	31.5232	31.5102	31.5104	0.2396	
3	30.0013	32.5822	31.9661	31.8874	31.8730	31.8734	0.2746	
4	30.9508	33.4068	32.8202	32.8212	32.8034	32.8071	0.2442	
			$K^{11}BO_2{\cdot}1.33H_2O$					
			170 ℃	208℃	208℃	208℃		
1	30.9503	33.5075	32.9787	32.9513	32.9419	32.9315	0.2253	
2	28.6208	31.4425	30.8841	30.8287	30.8195	30.8045	0.2261	
3	29.4854	32.2454	31.7081	31.6435	31.6355	31.6232	0.2254	0.2263
4	30.0015	33.2255	32.5852	32.5258	32.5098	32.5037	0.2239	

*, Mass loss as a fraction of the initial sample mass; **, Theoretical fraction of the mass that is H_2O in $K_2{}^{11}B_4O_7 \cdot 4H_2O$ and $K^{11}BO_2 \cdot 1.33H_2O$.

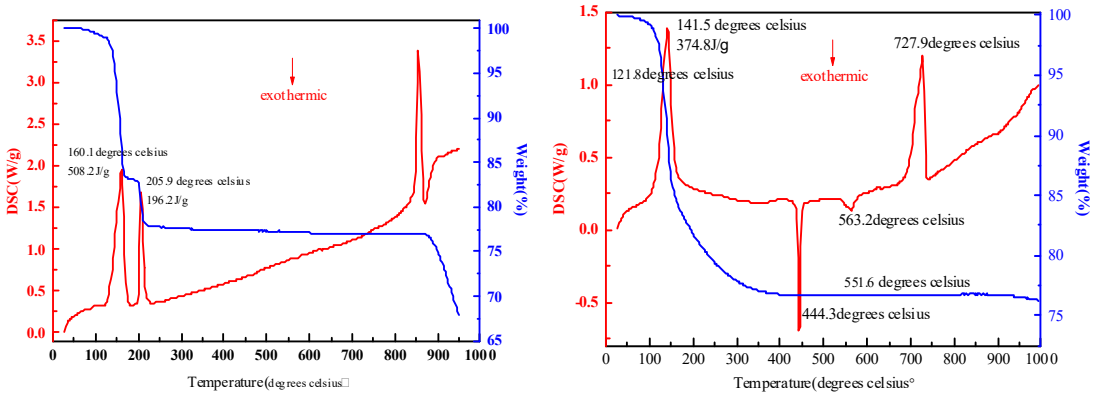

Figure S2. TGA and DSC of hydrous borates $KBO_2{\cdot}1.33H_2O$ (left panel) and $K_2B_4O_7{\cdot}4H_2O$ (right panel)

2 Characterization

A PANalytical X'pert Pro X-ray diffractometer using Kα radiation from an Rh-filtered Ag anode (λ=0.5609 Å) operating at 60 kV[S2] was used to characterise the hydrous crystals as shown in Figure S3. The measured diffraction patterns are compared with simulated[S3] diffraction patterns for crystal structure reports from the literature for $KBO_2{\cdot}1.33H_2O$ (ICSD_1235)[S4] and $K_2B_4O_7{\cdot}4H_2O$ (ICSD_34648).[S5] It can qualitatively be confirmed that the hydrous samples are $K^{11}BO_2{\cdot}1.33H_2O$ and $K_2{}^{11}B_4O_7{\cdot}4H_2O$.

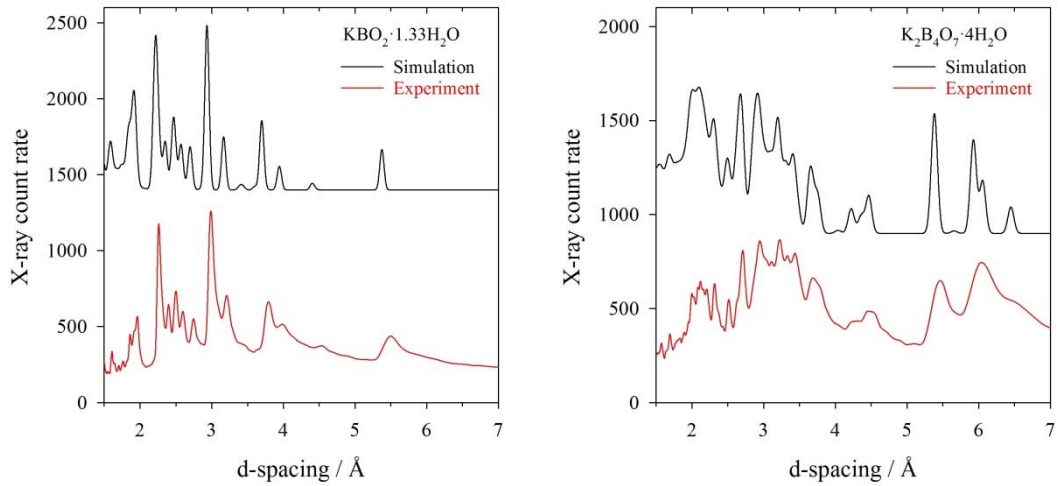

Figure S3 X-ray diffraction characterisation of the hydrous borate crystals $K^{11}BO_2{\cdot}1.33H_2O$ (left hand panel) and $K_2{}^{11}B_4O_7{\cdot}4H_2O$ (right hand panel). The lower red curves are experimental data, measured in a fused silica capillary on a PANalytical X'pert Pro X-ray diffractometer using Kα radiation from a Rh-filtered Ag anode (λ=0.5609 Å) operating at 60 kV. The upper black curves (displaced vertically for clarity) are simulations of the XRD patterns for the reported structures of $KBO_2{\cdot}1.33H_2O$[S4] (left hand panel) and $K_2B_4O_7{\cdot}4H_2O$[S5] (right hand panel). The simulations were calculated using CrystalMaker software,[S3] with a simple Gaussian broadening, sufficient to demonstrate that the expected hydrous borate crystal phase was prepared.

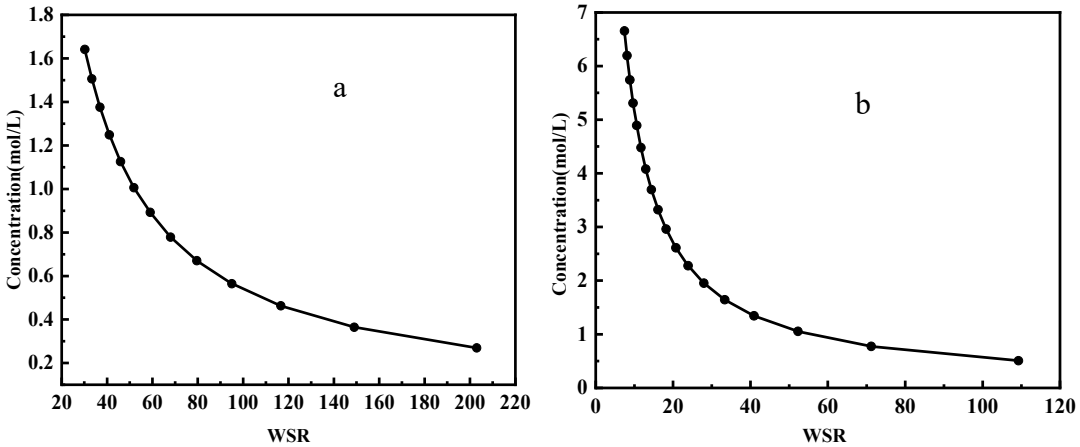

Figure S4 Relationship between water-salt molar ratio (WSR) and concentration (mol/L). a: low salt content, b: high salt content.

Table S3 Details of structural models of $B(OH)_3$ and $B(OH)_4^-$

	Point group	B-O/ Å	∠O-B-O/°	SPE/a.u.	Δ*E*/kJ/mol	
trans-$B(OH)_3$	C_{3h}	1.366	120.0	-252.4659	0	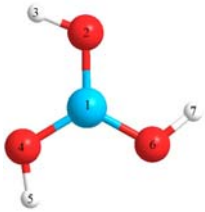
cis-$B(OH)_3$	*Cs*	$B_{(1)}$-$O_{(2)}$: 1.369 $B_{(1)}$-$O_{(6)}$: 1.366 $B_{(1)}$-$O_{(4)}$: 1.365	∠$O_{(2)}$-$B_{(1)}$-$O_{(6)}$: 125.4 ∠$O_{(2)}$-$B_{(1)}$-$O_{(4)}$: 118.8 ∠$O_{(6)}$-$B_{(1)}$-$O_{(4)}$: 115.8	-252.4637	5.8	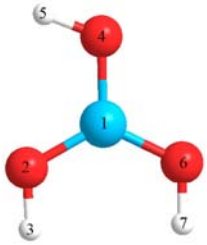
$B(OH)_4^-$	S_4	1.473	∠$O_{(8)}$-$B_{(1)}$-$O_{(6)}$:107.4 ∠$O_{(8)}$-$B_{(1)}$-$O_{(4)}$:113.7 ∠$O_{(8)}$-$B_{(1)}$-$O_{(2)}$:107.4 ∠$O_{(6)}$-$B_{(1)}$-$O_{(4)}$:107.4 ∠$O_{(6)}$-$B_{(1)}$-$O_{(2)}$:113.7 ∠$O_{(4)}$-$B_{(1)}$-$O_{(2)}$:107.4	-328.4238		

***trans*-$B(OH)_3(H_2O)_n$**

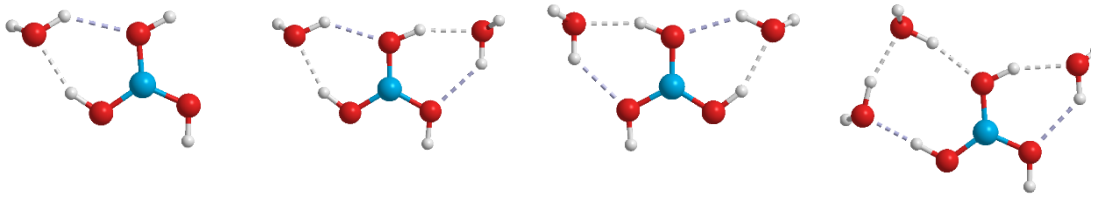

1-1 **2-1** 2-2 **3-1**

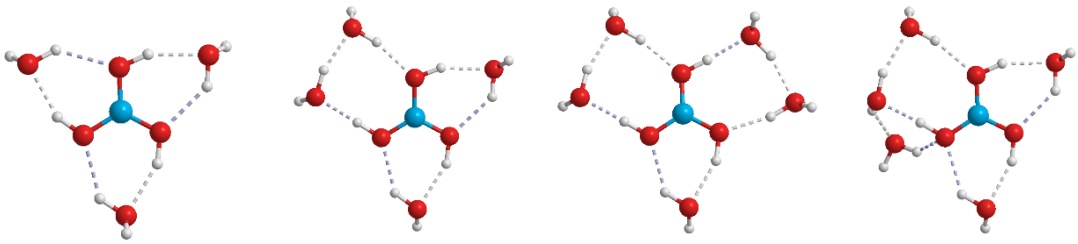

3-2 **4-1** **5-1** 5-2

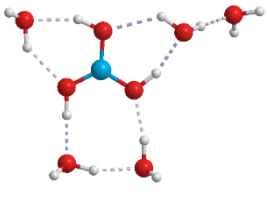

5-3

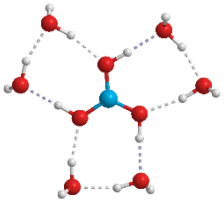

6-1

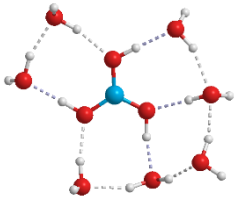

7-1

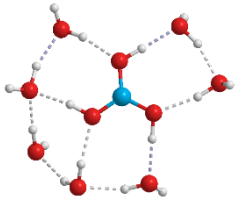

7-2

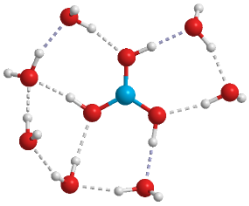

7-3

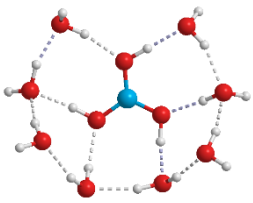

8-1

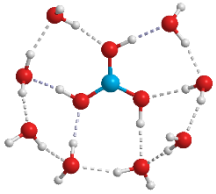

8-2

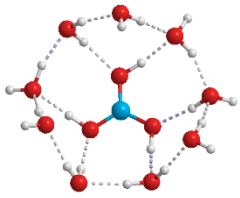

9-1

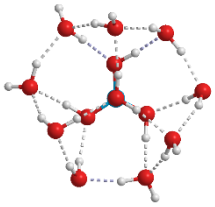

10-1

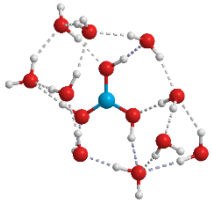

10-2

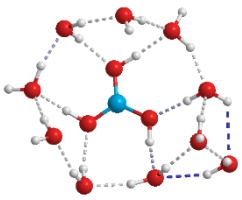

10-3

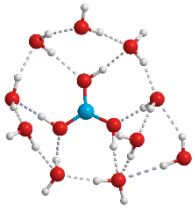

10-4

***cis*-B(OH)$_3$(H$_2$O)$_n$**

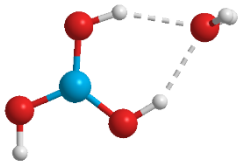

1-1

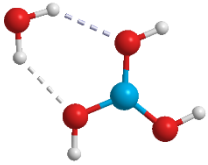

1-2

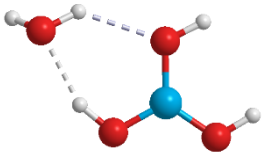

1-3

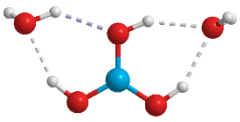

2-1

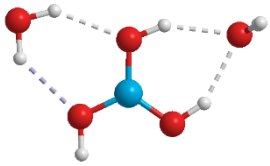

2-2

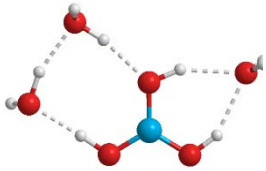

3-1

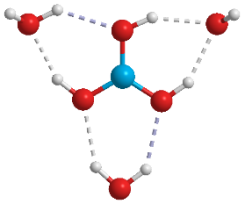

3-2

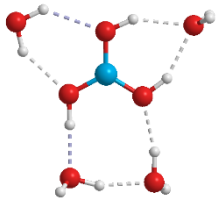

4-1

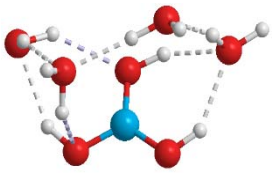

4-2

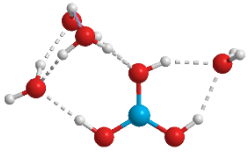

4-3

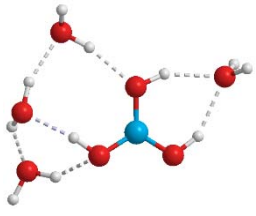

4-4

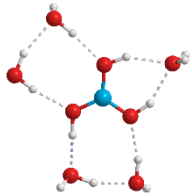

5-1

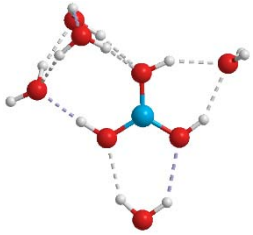

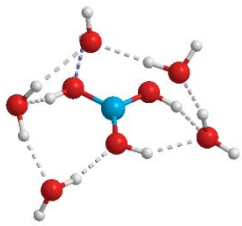

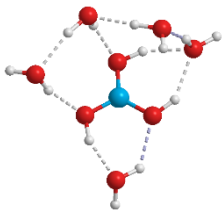

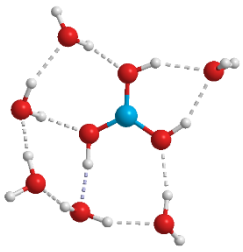

5-2 5-3 5-4 **6-1**

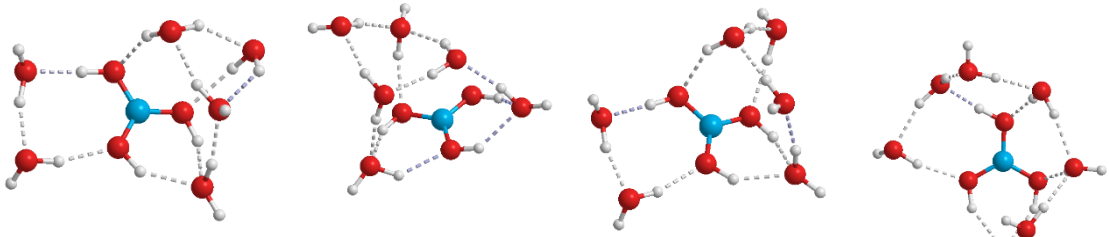

6-2 6-3 6-4 **7-1**

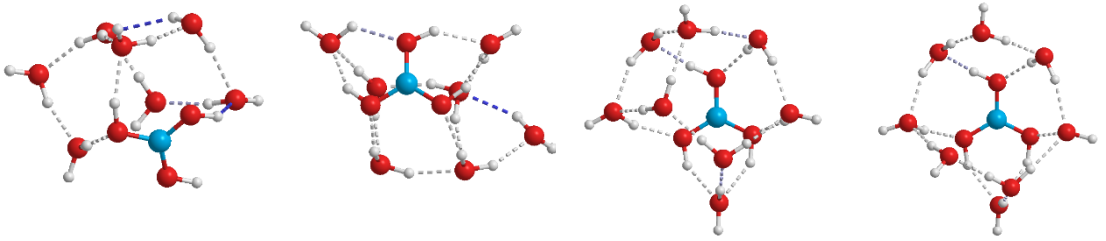

7-2 7-3 **8-1** 8-2

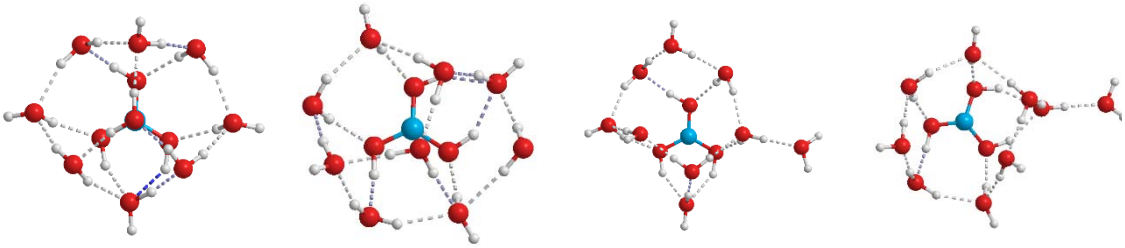

9-1 9-2 9-3 9-4

$B(OH)_4^-(H_2O)_n$

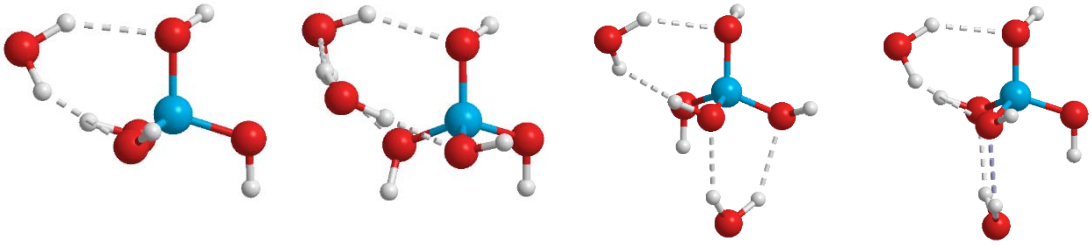

1-1 **2-1** 2-2 2-3

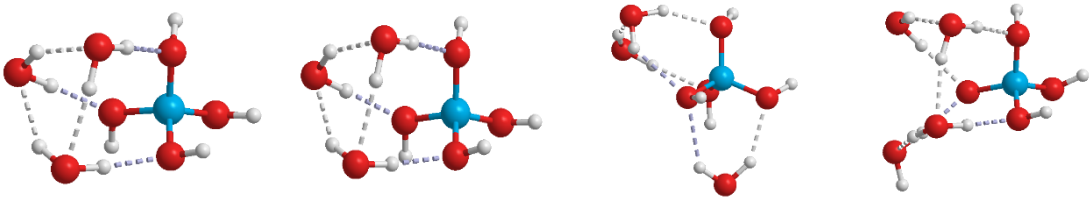

3-1 3-2 3-3 **4-1**

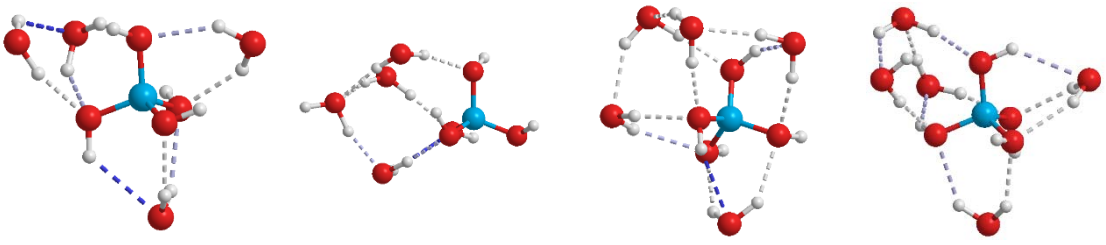

4-2 4-3 **5-1** 5-2

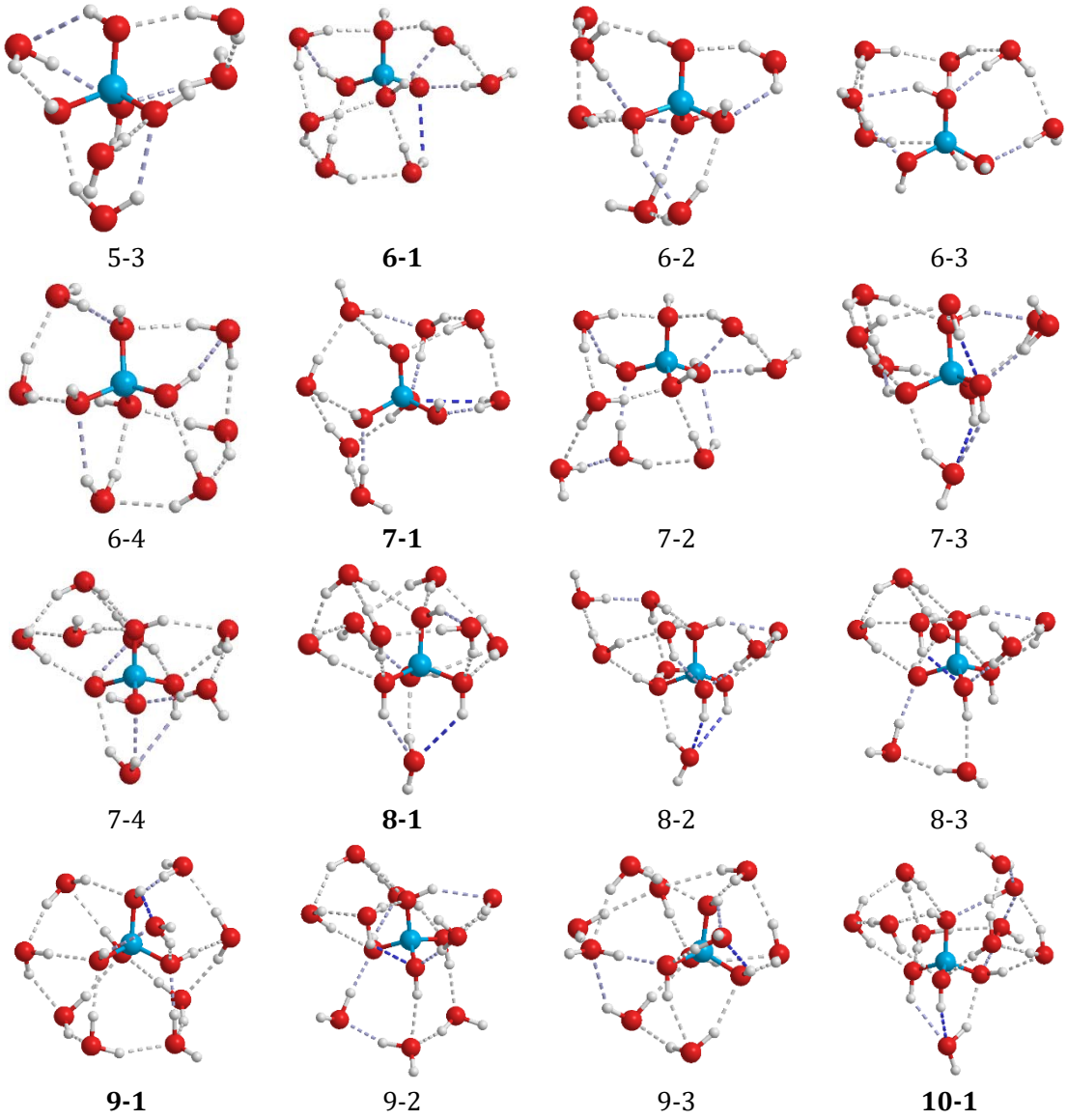

Figure S5 Optimized structures of $[B(OH)_3(H_2O)_n]$ and $[B(OH)_4^-(H_2O)_n]$ clusters

Table S4 Energy data for $[B(OH)_3(H_2O)_n]$ and $[B(OH)_4^-(H_2O)_n]$ clusters

n	E_0/a.u.	*E*/a.u.	*H*/a.u.	*G*/a.u.	ΔE_0/(kJ/mol)	ΔE/(kJ/mol)	ΔH/(kJ/mol)	ΔG/(kJ/mol)
				***trans*-B(OH)$_3$(H$_2$O)$_n$**				
1-1	**-328.8831**	**-328.8757**	**-328.8747**	**-328.9141**	-15.75	-15.23	-101.08	18.64
2-1	**-405.3017**	**-405.2912**	**-405.2903**	**-405.3370**	-35.18	-33.87	-122.61	34.13
3-1	**-481.7217**	**-481.7084**	**-481.7075**	**-481.7617**	-58.29	-56.97	-148.34	44.90
3-2	-481.7204	-481.7069	-481.7060	-481.7598	-54.87	-53.04	-144.40	49.88
4-1	**-558.1403**	**-558.1242**	**-558.1232**	**-558.1841**	-77.71	-76.40	-170.13	61.70
5-1	**-634.5605**	**-634.5417**	**-634.5408**	**-634.6091**	-101.34	-100.29	-196.91	71.68
5-2	-634.5557	-634.5363	-634.5354	-634.6039	-88.74	-86.12	-182.73	85.33

5-4	-634.5569	-634.5372	-634.5362	-634.6078	-91.89	-88.48	-184.84	75.09
6-1	**-710.9808**	**-710.9594**	**-710.9584**	**-711.0333**	-125.24	-124.71	-223.69	83.75
7-1	**-787.3996**	**-787.3753**	**-787.3743**	**-787.4561**	-145.19	-144.40	-246.01	99.51
7-2	-787.3990	-787.3748	-787.3739	-787.4549	-143.61	-143.09	-244.96	102.66
7-3	-787.3996	-787.3752	-787.3743	-787.4554	-145.19	-144.14	-246.01	101.34
8-1	**-863.8180**	**-863.7911**	**-863.7902**	**-863.8766**	-164.09	-163.83	-268.33	121.30
8-2	-863.8170	-863.7902	-863.7892	-863.8758	-161.47	-161.47	-265.70	123.40
9-1	**-940.2357**	**-940.2064**	**-940.2055**	**-940.2974**	-181.16	-181.95	-289.07	142.30
10-1	**-1016.664**	**-1016.633**	**-1016.632**	**-1016.722**	-226.06	-229.73	-339.21	153.33
10-2	-1016.6561	-1016.6245	-1016.6235	-1016.7183	-205.31	-207.41	-316.90	163.04
10-3	-1016.6522	-1016.6206	-1016.6196	-1016.7155	-195.07	-197.18	-306.66	170.39
10-4	-1016.6505	-1016.6186	-1016.6176	-1016.7150	-190.61	-191.92	-301.41	171.71
				***cis*-B(OH)$_3$(H$_2$O)$_n$**				
1-1	**-328.8836**	**-328.8758**	**-328.8749**	**-328.9153**	-22.84	-21.53	-24.15	9.45
1-2	-328.8792	-328.8720	-328.8711	-328.9094	-11.29	-11.55	-14.18	24.94
1-3	-328.8812	-328.8735	-328.8725	-328.9124	-16.54	-15.49	-17.85	17.07
2-1	**-405.3018**	**-405.2911**	**-405.2902**	**-405.3375**	-41.22	-39.65	-44.90	26.78
2-2	-405.3002	-405.2891	-405.2882	-405.3371	-37.02	-34.39	-39.65	27.83
3-1	**-481.7213**	**-481.7079**	**-481.7069**	**-481.7617**	-63.01	-61.70	-69.31	38.86
3-2	-481.7189	-481.7046	-481.7037	-481.7611	-56.71	-53.04	-60.91	40.43
4-1	**-558.1388**	**-558.1220**	**-558.1210**	**-558.1843**	-79.55	-76.66	-86.90	55.14
4-2	-558.1370	-558.1211	-558.1201	-558.1791	-74.83	-74.30	-84.54	68.79
4-4	-558.1373	-558.1210	-558.1200	-558.1806	-75.61	-74.04	-84.28	64.85
4-5	-558.1375	-558.1207	-558.1198	-558.1827	-76.14	-73.25	-83.75	59.34
5-1	**-634.5587**	**-634.5401**	**-634.5391**	**-634.6066**	-102.39	-102.13	-115.00	72.20
5-2	-634.5580	-634.5391	-634.5382	-634.6057	-100.56	-99.51	-112.63	74.56
5-3	-634.5578	-634.5391	-634.5382	-634.6052	-100.03	-99.51	-112.63	75.88
5-4	-634.5564	-634.5377	-634.5367	-634.6029	-96.36	-95.83	-108.70	81.92
6-1	**-710.9791**	**-710.9582**	**-710.9572**	**-711.0274**	-126.55	-127.60	-143.09	93.21
6-2	-710.9781	-710.9564	-710.9555	-711.0300	-123.92	-122.87	-138.63	86.38
6-3	-710.9762	-710.9548	-710.9538	-711.0265	-118.94	-118.67	-134.16	95.57
6-4	-710.9770	-710.9560	-710.9551	-711.0254	-121.04	-121.82	-137.58	98.46
7-1	**-787.3984**	**-787.3748**	**-787.3738**	**-787.4504**	-147.82	-149.13	-167.24	108.43
7-2	-787.3965	-787.3729	-787.3720	-787.4481	-142.83	-144.14	-162.52	114.47
7-3	-787.3954	-787.3719	-787.3709	-787.4467	-139.94	-141.51	-159.63	118.15
8-1	**-863.8252**	**-863.8001**	**-863.7992**	**-863.8779**	-188.77	-193.50	-214.50	111.85
8-2	-863.8202	-863.7942	-863.7934	-863.8770	-175.65	-178.01	-199.28	114.21
9-1	**-940.2417**	**-940.2140**	**-940.2131**	**-940.2982**	-202.69	-207.94	-231.57	134.16
9-2	-940.2401	-940.2119	-940.2110	-940.2962	-198.49	-202.43	-226.06	139.41
9-3	-940.2371	-940.2075	-940.2066	-940.2989	-190.61	-190.87	-214.50	132.33
9-4	-940.2368	-940.2071	-940.2061	-940.2991	-189.82	-189.82	-213.19	131.80
				B(OH)$_4^-$(H$_2$O)$_n$				
1-1	**-404.8444**	**-404.8345**	**-404.8431**	**-404.8768**	-24.42	-23.10	-50.93	11.29
2-1	**-481.2673**	**-481.2545**	**-481.2658**	**-481.3040**	-55.14	-53.56	-91.10	15.49

2-2	-481.2659	-481.2534	-481.2647	-481.3017	-51.46	-50.67	-88.22	21.53
2-3	-481.2660	-481.2534	-481.2647	-481.3021	-51.72	-50.67	-88.22	20.48
3-1	**-557.6912**	**-557.6763**	**-557.6897**	**-557.7306**	-88.48	-88.74	-134.43	21.27
3-2	-557.6911	-557.6763	-557.6896	-557.7305	-88.22	-88.74	-134.16	21.53
3-3	-557.6880	-557.6726	-557.6868	-557.7282	-80.08	-79.03	-126.81	27.57
4-1	**-634.1109**	**-634.0931**	**-634.1092**	**-634.1542**	-110.80	-110.80	-166.19	34.92
4-2	-634.1075	-634.0891	-634.1064	-634.1523	-101.87	-100.29	-158.84	39.91
4-3	-634.1088	-634.0910	-634.1073	-634.1521	-105.28	-105.28	-161.21	40.43
5-1	**-710.5318**	**-710.5117**	**-710.5303**	**-710.5773**	-136.26	-137.58	-202.16	49.88
5-2	-710.5297	-710.5093	-710.5283	-710.5763	-130.75	-131.28	-196.91	52.51
5-3	-710.5293	-710.5085	-710.5279	-710.5775	-129.70	-129.17	-195.86	49.36
6-1	**-786.9547**	**-786.9321**	**-786.9534**	**-787.0041**	-166.98	-169.08	-243.38	55.14
6-2	-786.9515	-786.9287	-786.9500	-787.0009	-158.58	-160.16	-234.46	63.54
6-3	-786.9536	-786.9306	-786.9517	-787.0034	-164.09	-165.14	-238.92	56.97
6-4	-786.9535	-786.9306	-786.9522	-787.0035	-163.83	-165.14	-240.23	56.71
7-1	**-863.3761**	**-863.3511**	**-863.3744**	**-863.4286**	-193.76	-196.91	-279.09	66.43
7-2	-863.3757	-863.3504	-863.3745	-863.4294	-192.71	-195.07	-279.35	64.32
7-3	-863.3747	-863.3494	-863.3736	-863.4269	-190.09	-192.45	-276.99	70.89
7-4	-863.3738	-863.3483	-863.3725	-863.4271	-187.72	-189.56	-274.10	70.36
8-1	**-939.7961**	**-939.7688**	**-939.7945**	**-939.8504**	-216.87	-221.33	-312.43	84.80
8-2	-939.7929	-939.7648	-939.7905	-939.8495	-208.46	-210.83	-301.93	87.17
8-3	-939.7942	-939.7661	-939.7927	-939.8516	-247.58	-252.31	-354.71	90.58
9-1	**-1016.219**	**-1016.189**	**-1016.218**	**-1016.277**	-237.87	-240.76	-344.20	95.31
9-2	-1016.2153	-1016.1846	-1016.2140	-1016.2752	-243.38	-250.47	-274.36	96.62
9-3	-1016.2174	-1016.1883	-1016.1874	-1016.2747	-243.38	-250.47	-274.36	96.62
10-1	-1092.6383	-1092.6055	-1092.6371	-1092.6995	-268.85	-273.58	-385.42	107.12

(1 a.u.= 2625.5 kJ/mol)

E_0, E, H, and G were computed according to following equations:

$$\Delta E_0 = \{E_0(\mathrm{M}) + E_{0_{\mathrm{H2O}}} \times n - E_{0_{\mathrm{B(OH)_3(H2O)}_n}}\}$$

$$\Delta E = \{E(\mathrm{M}) + E_{\mathrm{H2O}} \times n - E_{\mathrm{B(OH)_3(H2O)}_n}\}$$

$$\Delta H = \{H(\mathrm{M}) + H_{\mathrm{H2O}} \times n - H_{\mathrm{B(OH)_3(H2O)}_n}\}$$

$$\Delta E = \{G(\mathrm{M}) + G_{\mathrm{H2O}} \times n - G_{\mathrm{B(OH)_3(H2O)}_n}\}$$

M = *trans*-$B(OH)_3$, *cis*-$B(OH)_3$, $B(OH)_4^-$

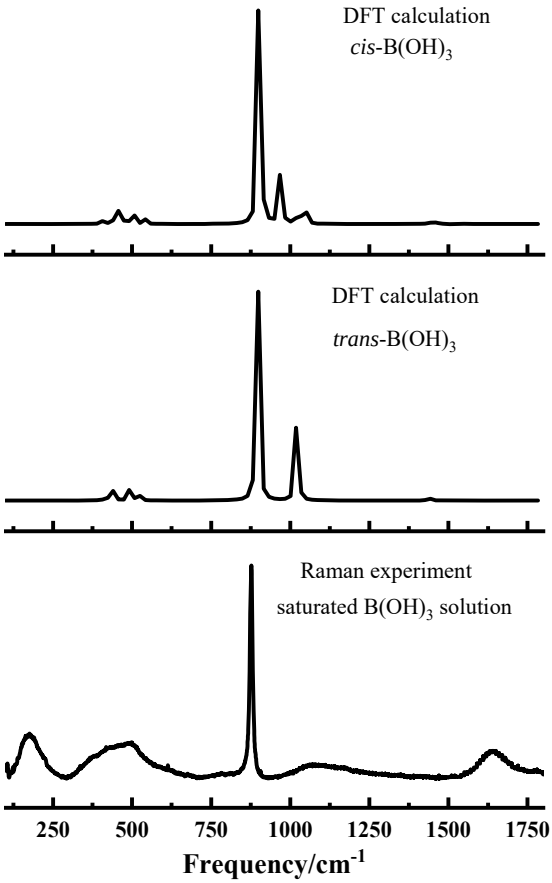

Figure S6 Calculated and experimental Raman spectra of aqueous $B(OH)_3$ solution

aqueous $K_2B_4O_7$ solutions for WSR=100

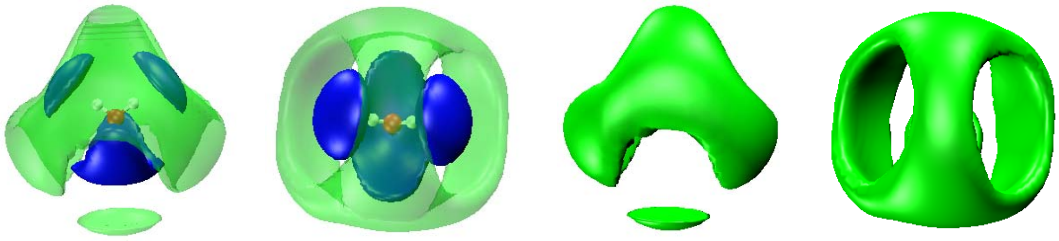

a b c d

aqueous $K_2B_4O_7$ solutions for WSR=60

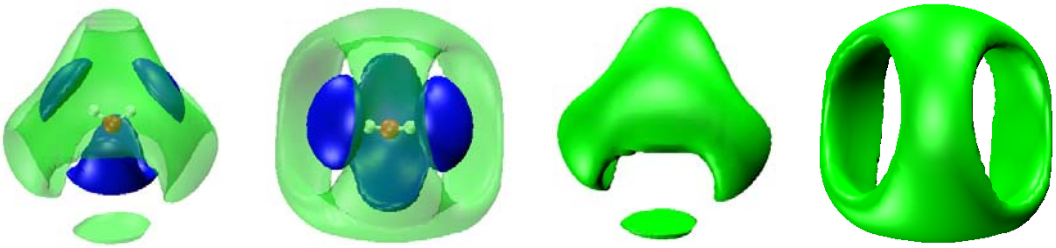

a b c d

aqueous KBO_2 solutions for WSR=60

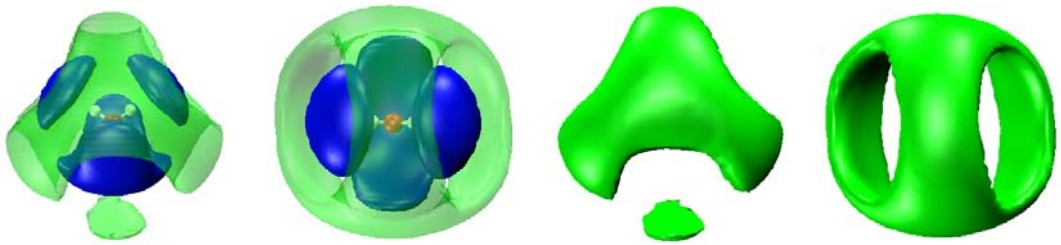

aqueous KBO_2 solutions for WSR=20

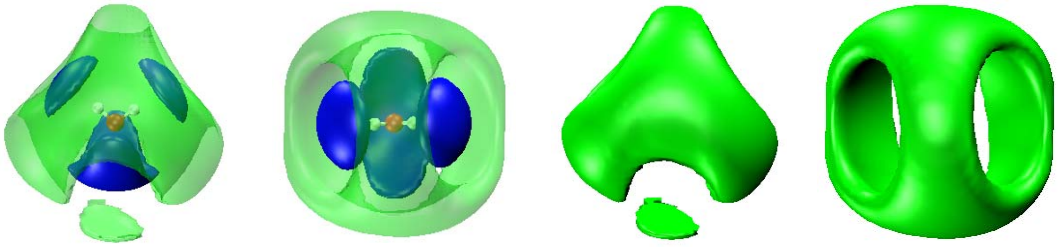

Figure S7 Spatial density functions of neighboring water molecules with respect to the central water molecule. The dark blue lobes represent the first coordination sphere, and the light green and semitransparent lobes/green lobes represent the second sphere. The red and white balls in the center represent the O and H atoms of H_2O, respectively. (a): side view, (b): top view; (c): side view of the second hydration sphere of water; (d): top view of the second hydration sphere of water.

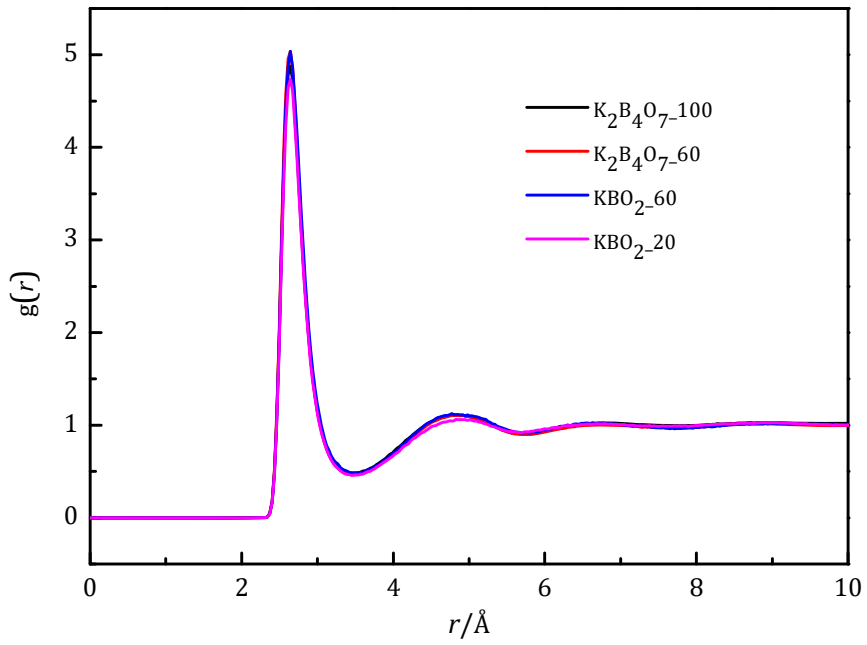

Figure S8 Pair distribution functions of K–O(W) at various concentrations obtained using EPSR modeling

trans-$B(OH)_3$_monodentate

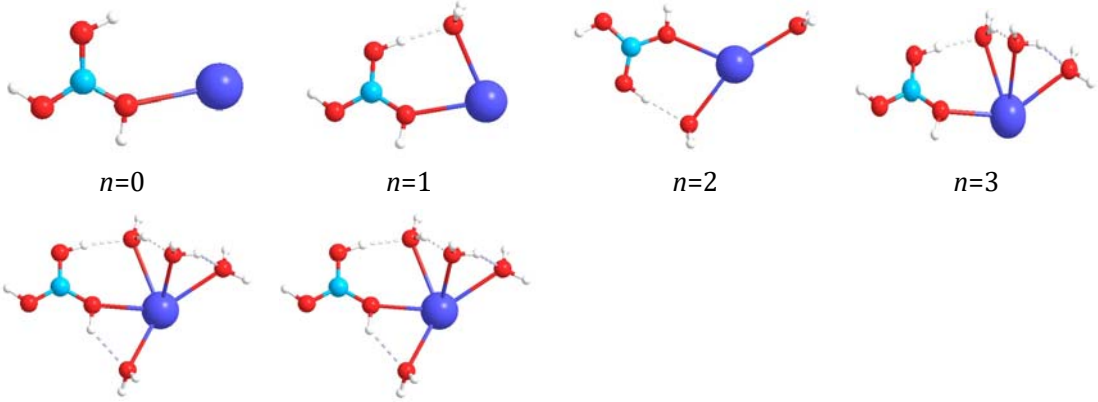

n=0 *n*=1 *n*=2 *n*=3

n=4 *n*=5

cis-$B(OH)_3$_monodentate

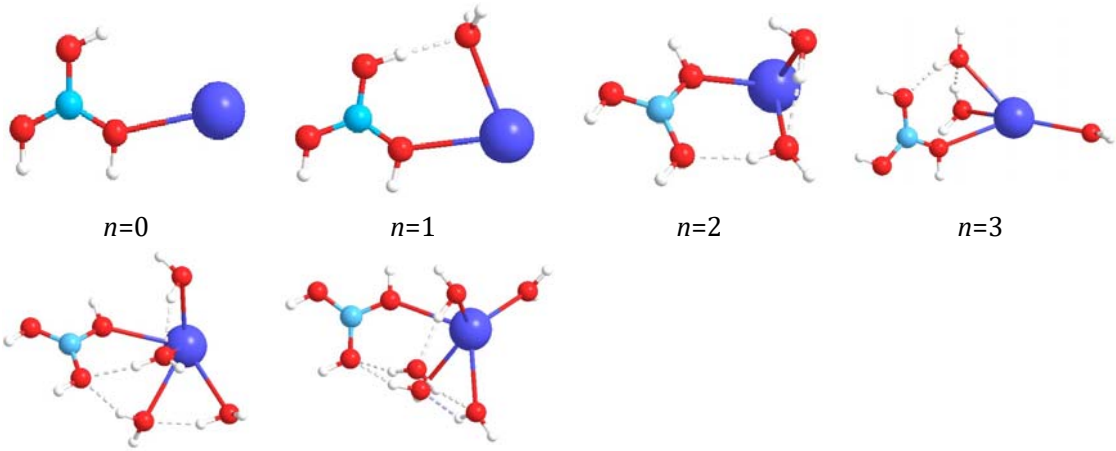

n=0 *n*=1 *n*=2 *n*=3

n=4 *n*=5

cis-$B(OH)_3$_bidentate

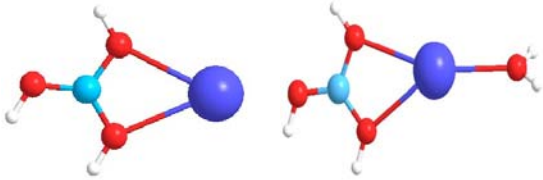

n=0 *n*=1

Figure S9 Optimized structures of $[KB(OH)_3(H_2O)_n]^+$ and $[KB(OH)_4(H_2O)_n]$

Table S5 Energy and structural parameters of $[KB(OH)_3(H_2O)_n]^+$ and $[KB(OH)_4(H_2O)_n]$

n	E_0/a.u.	E/a.u.	H/a.u.	G/a.u.	ΔE_0/(kJ/mol)	ΔE/(kJ/mol)	ΔH/(kJ/mol)	ΔG/(kJ/mol)	$r_{K\text{-}B}$/Å	$r_{K\text{-}O}$/Å	$r_{K\text{-}O(W)}$/Å
					***trans*-B(OH)$_3$_monodentate**						
0	-852.3374	-852.3307	-852.3298	-852.3696					3.897	2.748	
1	-928.7590	-928.7493	-928.7484	-928.7950	-27.31	-26.78	-29.41	8.93	3.819	2.737	2.749
2	-1005.1741	-1005.1603	-1005.1594	-1005.2169	-37.54	-33.61	-38.86	27.04	3.838	2.744	2.722
3	-1081.5959	-1081.5807	-1081.5798	-1081.6382	-65.37	-65.11	-72.98	46.73	3.820	2.731	2.789
4	-1158.0133	-1157.9935	-1157.9926	-1158.0630	-81.65	-76.66	-87.16	57.23	3.885	2.680	2.825
5	-1234.4318	-1234.4094	-1234.4084	-1234.4853	-100.82	-96.3559	-109.22	74.30	3.809	2.705	2.80
					***cis*-B(OH)$_3$_monodentate**						
0	-852.3393	-852.3325	-852.3316	-852.3717					3.917	2.765	
1	-928.7561	-928.7464	-928.7455	-928.7919	-14.70	-14.44	-17.06	22.57	3.837	2.746	2.743
2	-1005.1741	-1005.1612	-1005.1603	-1005.2144	-32.56	-31.24	-36.49	39.12	3.883	2.770	2.749
3	-1081.5895	-1081.5722	-1081.5713	-1081.6373	-43.58	-38.07	-45.94	54.61	3.916	2.801	2.747
4	-1158.0097	-1157.9904	-1157.9895	-1158.0567	-67.21	-63.80	-74.30	79.29	3.897	2.785	2.770
5	-1234.4268	-1234.4039	-1234.4029	-1234.4815	-82.70	-77.19	-90.05	89.79	3.889	2.776	2.758
					***cis*-B(OH)$_3$_bidentate**						
0	-852.3346	-852.3280	-852.3271	-852.3662					3.261	2.757	
1	-928.7542	-928.7435	-928.7425	-928.7923	-22.05	-18.64	-21.0	7.09	3.272	2.771	2.691

(1 a.u.= 2625.5 kJ/mol)

E_0, E, H, and G were computed according to following equations:

$$\Delta E_0 = \{E_0(\mathrm{M}) + E_{0_{\mathrm{H2O}}} \times n - E_{0_{\mathrm{KB(H2O)}_n}}\};\ \Delta E = \{E(\mathrm{M}) + E_{\mathrm{H2O}} \times n - E_{\mathrm{KB(H2O)}_n}\};\ \Delta H = \{H(\mathrm{M}) + H_{\mathrm{H2O}} \times n - H_{\mathrm{KB(H2O)}_n}\}$$

$$\Delta E = \{G(\mathrm{M}) + G_{\mathrm{H2O}} \times n - G_{\mathrm{KB(H2O)}_n}\}$$

M is the ion pair between K^+ and $B(OH)_3$

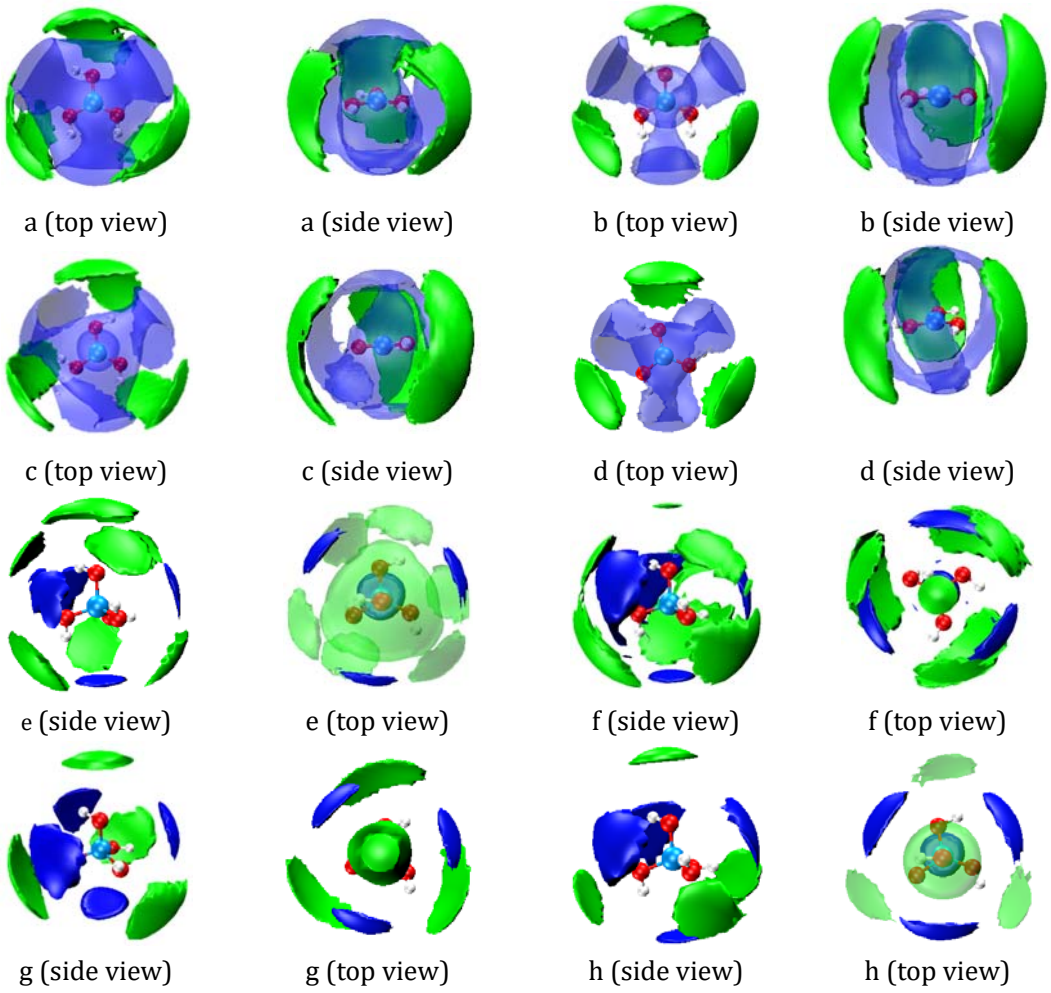

Figure S10 Spatial density function surfaces showing the probability density for correlations of hydration water molecules with respect to the central [$B(OH)_3$] and [$B(OH)_4^-$] moieties. The blue and semitransparent lobes represent water molecules in the first (direct) hydration shell, whilst the green lobes represent water molecules in the second (indirect) hydration shell. For the first and second hydration shells, the isosurfaces have been selected to show the distribution of neighbours with the threshold selected to show the most probable 30% and 20% of neighbour locations respectively. a, b: the *cis*-$B(OH)_3$ in aqueous $K_2B_4O_7$ solutions with WSR = 100 and 60; c, d: the *trans*-$B(OH)_3$ in aqueous $K_2B_4O_7$ solutions with WSR = 100 and 60; e, f: the $B(OH)_4^-$ anion in aqueous $K_2B_4O_7$ solutions with WSR= 100 and 60; g, h: the $B(OH)_4^-$ anion in aqueous KBO_2 solutions with WSR=60 and 20; the pink, red, and white balls in the center respectively represent B, O, and H atoms of $B(OH)_3$ or $B(OH)_4^-$. The first (direct) hydration shell of $B(OH)_3$ is in the range 2.6 to 4.5 Å, and the second shell is in the range 4.6 to 5.2 Å. The first (direct) hydration shell of $B(OH)_4^-$ is in the range 2.6 to 3.9 Å, and the second shell is in the range 3.7 to 4.8 Å.

Table S6 Structural parameters of $[B(OH)_3(H_2O)_n]$ and $[B(OH)_4^-(H_2O)_n]$ clusters

Species	*n*	B-O	B-O(W)$_{dir}$	B-O(W)$_{inter}$	B-O(W)$_{axial}$	O(B)-O(W)	O(W)-O(W)
	1	1.367	3.227			2.803	
	2	1.367	3.218			2.796	
	3	1.367	3.511			2.76	2.725
	4	1.367	3.430			2.764	2.723

trans-$B(OH)_3(H_2O)_n$	5	1.367	3.564			2.742	2.72
	6	1.367	3.653			2.721	2.715
	7	1.367	3.631	4.593		2.71	2.79
	8	1.367	3.626	4.469		2.727	2.794
	9	1.367	3.625	4.446		2.753	2.786
	10	1.367	3.619	4.167	2.729	2.755	2.782
	11	1.367	3.628	4.576		2.757	2.824
	1	1.367	3.224			2.849	
	2	1.368	3.234			2.825	
	3	1.368	3.534			2.796	2.732
	4	1.368	3.476			2.816	2.724
cis-$B(OH)_3(H_2O)_n$	5	1.367	3.630			2.798	2.791
	6	1.368	3.558	4.494		2.792	2.78
	7	1.369	3.488	4.303		2.769	2.782
	8	1.369	3.489	3.884		2.755	2.782
	9	1.368	3.521	4.191	4.401	2.795	2.802
	9	1.368	3.478	4.21			
	1	1.473	3.077			2.807	
	2	1.473	3.359			2.768	2.909
	3	1.473	3.570			2.713	2.924
	4	1.473	3.650			2.754	2.849
	5	1.473	3.336			2.838	2.897
$B(OH)_4^-(H_2O)_n$	6	1.473	3.415			2.835	2.873
	7	1.473	3.537			2.801	2.820
	8	1.473	3.421			2.830	2.874
	9	1.473	3.488			2.810	2.841
	10	1.473	3.482	4.595		2.812	2.839

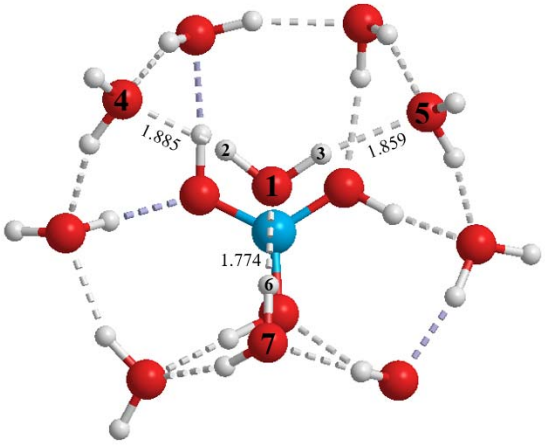

Figure S11 Minimum energy configuration of $B(OH)_3(H_2O)_{10}$

Table S7 B-O(W) and hydrogen bond values of $B(OH)_3(H_2O)_{10}$ during the structural optimization

optimization step	B-O(W)	$O_{(4)}...H_{(2)}$	$O_{(5)}...H_{(3)}$	$O_{(1)}...H_{(6)}$
0	4.241	2.377	2.357	2.0
7	3.226	1.958	2.596	2.169
14	2.920	1.922	1.916	1.928
28	2.735	1.882	1.861	1.776
40	2.728	1.882	1.859	1.775
50	2.729	1.882	1.861	1.775
final step	2.729	1.884	1.859	1.774

Definition of reduced density gradient (RDG)

$$\mathrm{RDG}(r) = \frac{1}{2(3\pi^2)^{1/3}} \frac{|\nabla\rho(r)|}{\rho(r)^{4/3}}$$

where ∇ is the gradient operator. $|\nabla\rho(\mathrm{r})|$ is the magnitude of the electron density gradient.

$$\Omega(r) = sign[\lambda_2(r)]\rho(r)$$

where λ_2 is the second eigenvalue of three eigenvalues. $sign(\lambda_2)$ is the sign of the second largest eigenvalue of the electron density Hessian matrix λ_2 at position *r*. *sign* is the symbol (+/-) of the eigenvalue. $\rho(r)$ is the electron density at position *r*, which reflects the interaction intensity.

References

(S1) P. Toledano and A. Benhassaine, *Rev. Chim. Minér.*, 1970**, 7**, 287-291.

(S2) A. K. Soper and E. R. Barney, *J. Appl. Cryst.*, 2011**, 44**, 714-726.

(S3) D. C. Palmer, *Z. Kristallogr.*, 2015**, 230**, 559-572.

(S4) J. R. Clark and C. L. Christ, *Acta Cryst. B*, 1977**, 33**, 3272-3273.

(S5) M. Marezio, H. A. Plettinger and W. H. Zachariasen, *Acta Cryst.*, 1963**, 16**, 975-980.